Distinct and Cooperative Roles of *amh* and *dmrt1* in Self-Renewal and Differentiation of Male Germ Cells in Zebrafish

Qiaohong Lin,* Jie Mei,*,[1] Zhi Li,[†] Xuemei Zhang,* Li Zhou,[†] and Jian-Fang Gui*,[†],[1]
*College of Fisheries, Key Laboratory of Freshwater Animal Breeding, Ministry of Agriculture, Huazhong Agricultural University, Wuhan 430070, China and [†]State Key Laboratory of Freshwater Ecology and Biotechnology, Institute of Hydrobiology, Chinese Academy of Sciences, University of the Chinese Academy of Sciences, Wuhan 430072, China

ABSTRACT Spermatogenesis is a fundamental process in male reproductive biology and depends on precise balance between self-renewal and differentiation of male germ cells. However, the regulative factors for controlling the balance are poorly understood. In this study, we examined the roles of *amh* and *dmrt1* in male germ cell development by generating their mutants with Crispr/Cas9 technology in zebrafish. *Amh* mutant zebrafish displayed a female-biased sex ratio, and both male and female *amh* mutants developed hypertrophic gonads due to uncontrolled proliferation and impaired differentiation of germ cells. A large number of proliferating spermatogonium-like cells were observed within testicular lobules of the *amh*-mutated testes, and they were demonstrated to be both Vasa- and PH3-positive. Moreover, the average number of Sycp3- and Vasa-positive cells in the *amh* mutants was significantly lower than in wild-type testes, suggesting a severely impaired differentiation of male germ cells. Conversely, all the *dmrt1*-mutated testes displayed severe testicular developmental defects and gradual loss of all Vasa-positive germ cells by inhibiting their self-renewal and inducing apoptosis. In addition, several germ cell and Sertoli cell marker genes were significantly downregulated, whereas a prominent increase of Insl3-positive Leydig cells was revealed by immunohistochemical analysis in the disorganized *dmrt1*-mutated testes. Our data suggest that *amh* might act as a guardian to control the balance between proliferation and differentiation of male germ cells, whereas *dmrt1* might be required for the maintenance, self-renewal, and differentiation of male germ cells. Significantly, this study unravels novel functions of *amh* gene in fish.

KEYWORDS *amh*; *dmrt1*; germ cells; self-renewal; differentiation; Genetics of Sex

MALE sex determination is initiated by sex-determining genes that activate downstream factors essential for testis development and spermatogenesis, such as *amh*, *dmrt1*, and *sox9* (Herpin and Schartl 2015; Mei and Gui 2015). Spermatogenesis is a dynamic process, including self-renewal of spermatogonia via mitotic division, meiotic division of spermatocytes, and metamorphosis of spermatids (Xu *et al.* 2010). In the seminiferous tubules where spermatozoa are produced, the chief cells are male germ cells and Sertoli cells (Rossitto *et al.* 2015). Male germ cells are able to differentiate into spermatozoa, and their development relies on the direct membrane contact with Sertoli cells or paracrine signals secreted by Sertoli cells, such as bone morphogenetic proteins that are members of the transforming growth factor β (Tgfβ) family (Saitou 2009; Dimitriadis *et al.* 2015; Wang *et al.* 2016).

The subtle balance between self-renewal and differentiation of male germ cells is essential for normal male reproductive development and function, loss of which usually leads to male infertility (Rossitto *et al.* 2015). In mammals, germ cell maintenance requires some factors produced by Sertoli cells including *GDNF* and *cyp26b1* (Meng *et al.* 2000; Bowles *et al.* 2006), and other important factors expressed in spermatogonial stem cells, such as *plzf*, *nanos2*, and *dmrt1* (Tsuda *et al.* 2003; Buaas *et al.* 2004; Zhang *et al.* 2016). Follicle-stimulating hormone is a principal hormonal regulator of spermatogenesis and its receptor is also expressed by Sertoli cells (Marshall *et al.* 1995). Importantly, mutation of follicle-stimulating hormone

doi: https://doi.org/10.1534/genetics.117.300274
Manuscript received March 15, 2017; accepted for publication September 8, 2017; published Early Online September 11, 2017.
Supplemental material is available online at www.genetics.org/lookup/suppl/doi:10.1534/genetics.117.300274/-/DC1.
[1]Corresponding authors: College of Fisheries, Huazhong Agricultural University, No. 1 Shizishan St., Hongshan District, Wuhan 430070, Hubei, China. E-mail: jmei@mail.hzau.edu.cn; and Institute of Hydrobiology, Chinese Academy of Sciences, 7 Donghu South Rd., Wuhan 430072, Hubei, China. E-mail: jfgui@ihb.ac.cn

receptor (*fshr*) led to female-to-male sex reversal, whereas double mutation of *fshr* and LH receptor gene (*lhcgr*) resulted in infertile males in zebrafish (Zhang *et al.* 2015b).

In teleost fish, *amh*, *dmrt1*, and their orthologs had been observed to involve male sex determination and spermatogenesis (Xia *et al.* 2007; Li *et al.* 2014a,b). *Amh*, a member of the *Tgfb* superfamily, was shown to express in Sertoli cells and to be responsible for regression of Müllerian ducts in mammals (Kobayashi *et al.* 2011). *Amh* orthologs were widely identified in teleost fish. In medaka, *amh* expression was observed to start from somatic gonadal mesoderm when the migrating PGCs meet with somatic gonadal precursors (Nakamura *et al.* 2006). In zebrafish, *amh* was revealed to preferentially localize in Sertoli cells around type A spermatogonia, whereas its expression weakened and finally became absent when the primary spermatogonia differentiated, suggesting that *amh* in Sertoli cells might inhibit differentiation of male germ cells (Skaar *et al.* 2011). *Dmrt1* orthologs were also investigated in the model fish. *Dmy*, the duplicate of *dmrt1*, was confirmed as male sex-determining gene in medaka (Matson and Zarkower 2012). And, *dmrt1* mutation was revealed to lead a male-to-female sex reversal in the XY mutant gonads (Masuyama *et al.* 2012). In zebrafish, *dmrt1* was found to express in both germ line and Sertoli cells of the testes, and its mutation generated by TALEN technology was recently demonstrated to lead to testis development defects and female-biased sex ratio (Webster *et al.* 2017). However, the functional and cooperative roles between *amh* and *dmrt1* in germ cell development remained largely unclear *in vivo*. Here, we used CRISPR/Cas9 technology (Li and Wang 2017; Xiong *et al.* 2017) to construct *amh* and *dmrt1* mutants and thereby investigate the functional roles and regulative mechanisms of *amh* and *dmrt1* in male germ cell development.

Materials and Methods

Zebrafish lines and maintenance

AB line zebrafish used in this study were reared in the zebrafish facility of the Institute of Hydrobiology, Chinese Academy of Sciences. The maintenance, breeding, and staging of zebrafish were performed according to standard methods (Kimmel *et al.* 1995; Westerfield 2000). The use of zebrafish was approved by the Animal Research and Ethics Committees of the Institute of Hydrobiology.

Targeted gene disruption by CRISPR/ Cas9

Gene knockout by CRISPR/Cas9 was performed as described (Xiong *et al.* 2017). The guide RNA (gRNA) target sites were designed with an online tool, ZIFIT Targeter (http://zifit.partners.org/ZiFiT/CSquare9Nuclease.aspx), and gRNA was transcribed with the TranscriptAid T7 High-Yield Transcription Kit (Thermo Fisher Scientific, Waltham, MA). For Cas9 messenger RNA (mRNA) synthesis, pCS2-Cas9 expression vector was linearized with *Xba*I, purified, and transcribed using the mMESSAGE mMACHINE T7 ULTRA kit (Ambion) according to the manufacturer's instructions. Cas9 mRNA (300 ng/μl) and gRNA (20 ng/μl) were co-injected into one-cell-stage zebrafish embryos, and the mutations were analyzed by genomic PCR and sequencing (primers used were listed in Supplemental Material, Table S1 in File S1) as described (Yang *et al.* 2017).

Fertilization assessment

Fertilization rate assessment of male zebrafish was performed as described (Brion *et al.* 2004) with minor modifications. In the morning, *dmrt1* and *amh* mutant male zebrafish were crossed with wild-type (WT) females, respectively. After breeding, the eggs were collected, and the total number of embryos were recorded and placed in the incubator. The unfertilized eggs and dead embryos were counted and removed out at 4 and 24 hr postfertilization. Fertilization rate is the number of fertilized embryos divided by the total embryos, in percentage. Each experiment was performed more than three times.

Tissue collection and histological analysis

For histological analysis, intact testes at different developmental stages were carefully dissected after anesthetization and fixed in 4% paraformaldehyde for up to 24 hr at 4°, dehydrated, and embedded in paraffin. Testes were sectioned at 4-μm thickness and stained with hematoxylin and eosin (H&E) following the manufacturer's instructions. Histological analyses and the staging of spermatogenesis were performed as described previously (Leal *et al.* 2009; Sun *et al.* 2013). Each experiment was performed on at least three individual zebrafish in triplicate, and a series of sections was observed.

Antibody preparation and immunofluorescence analysis

The partial ORF of *insl3* was fused with pET-21b (Novagen) and the recombinant fusion protein was expressed in *Escherichia coli*. After purification, the expressed protein (1 μg/μl) was emulsified in isopyknic Freund's complete adjuvant (Sigma, St. Louis, MO) and injected into the lymph of rabbits. Two weeks later, the rabbits were subcutaneously booster immunized three times every 14 days, with equal purified protein emulsified in Freund's incomplete adjuvant. Ten days later, antiserum was collected and stored at −80° as described (Peng *et al.* 2009; Li *et al.* 2017).

WT and mutant testes at different stages were collected and fixed as above. After deparaffinization, slides were rehydrated in PBS for 20 min, repaired in EDTA antigen retrieval buffers, and incubated for 1 hr with 5% defatted milk diluted in PBS at room temperature to avoid nonspecific binding of antibodies. Then, slides were incubated overnight at 4° with primary antibodies: anti-Vasa antibody (rabbit, 1:50) (Liu *et al.* 2015), anti-Insl3 antibody (rabbit, 1:100), phosphohistone 3 (PH3) antibody (rabbit, 1:1000) (3377S, Cell Signaling Technology, Danvers, MA), anti-Sycp3 antibody (rabbit, 1:200) (ab150292) diluted in 1% defatted milk in PBS. After washing, the slides were incubated for 1 hr with (FITC)- or tetramethyl rhodamin isothiocyanate (TRITC)-conjugated secondary antibody (1: 150) (Thermo Fisher Scientific) in the

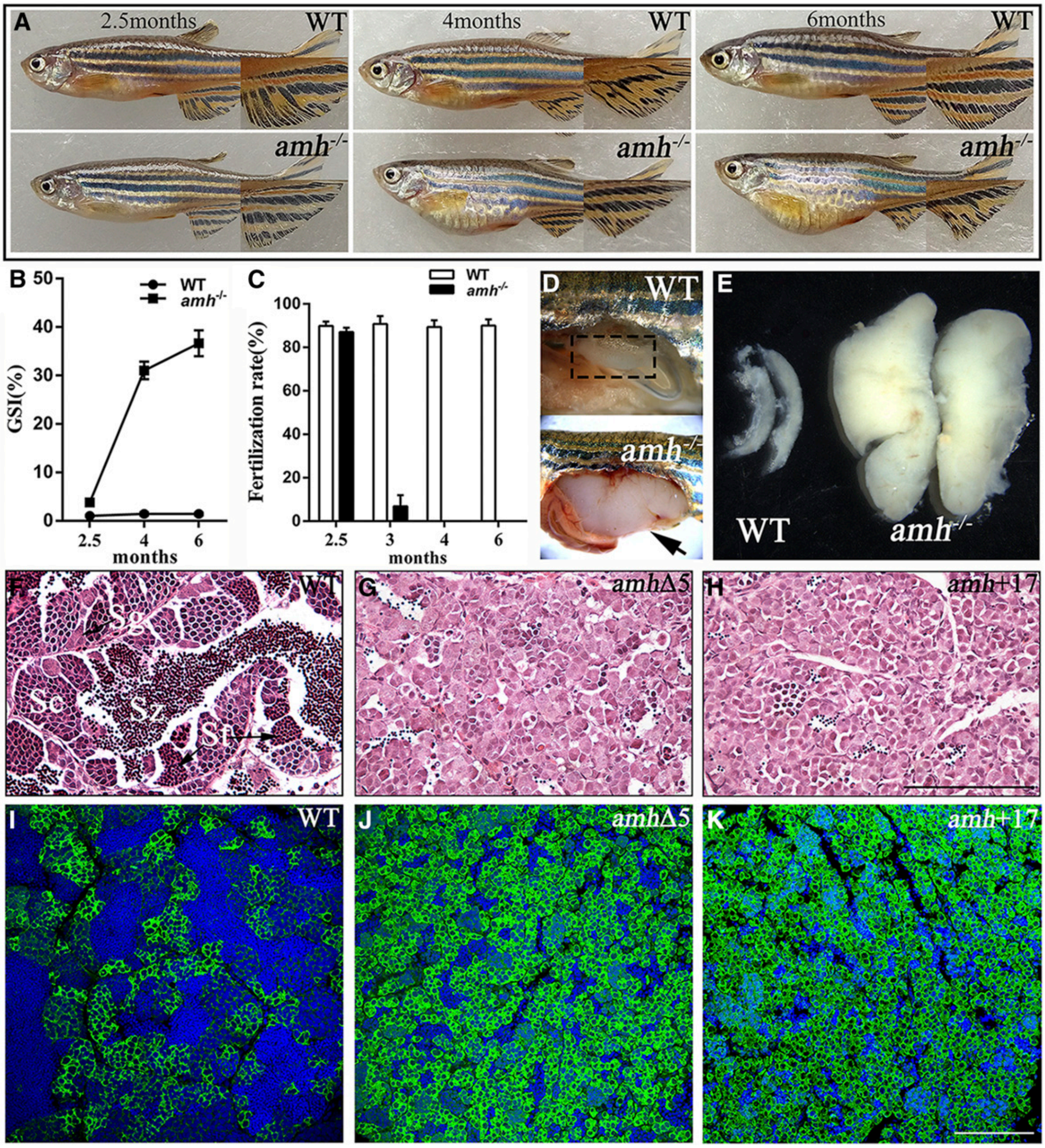

Figure 1 Loss of *amh* leads to the dysregulation of male germ cell development. (A) Comparison of the body shape and fin pigmentation between WT males and *amh* mutant males ($amh^{-/-}$) at 2.5, 4, and 6 months of age. (B) Gonadosomatic index (GSI = gonad weight / total body weight, in percentage) changes of WT and *amh* mutant males at 2.5, 4, and 6 months of age (mean ± SD, $n = 6$). (C) Fertilization rate changes of WT and *amh* mutant male zebrafish by crossing with WT female at 2.5, 3, 4, and 6 months of age (mean ± SD, $n = 5$). (D) Anatomical observation of WT and *amh* mutant testes (arrows). (E) Morphological comparison of WT and *amh* mutant testes. (F–H) Histological comparisons of testes from WT, *amh*Δ5, and *amh*+17 by H&E staining at 6 months of age. (I–K) Immunofluorescence of testis sections stained with anti-Vasa antibody at 6 months of age. Sg, spermatogonia; Sc, spermatocytes; St, spermatids; Sz, spermatozoa. Bar, 100 μm.

dark at room temperature. Finally, the samples were counterstained with DAPI (Sigma) to visualize cell nuclei and photographed using a Leica SP8 confocal microscope (Leica, Jena, Germany).

Probe synthesis and in situ hybridization

Zebrafish *nanos2* complementary DNA (cDNA) fragment was amplified by specific primers with a T7 RNA polymerase promoter (Table S1 in File S1) and a DIG RNA labeling kit (Roche, Mannheim, Germany) was used for probe synthesis. The intact testes were fixed with 4% paraformaldehyde in PBS at 4° overnight and immersed in 30% saccharose-PBS for up to 24 hr at 4°. Then the samples were embedded in optimal cutting temperature (OCT) and sectioned at 7-μm thickness with freezing microtome (Leica). After drying at 37° for 1 hr, the sections were stored at −80°. The mRNA detection by *in situ* hybridization was performed as previously described (Wang *et al.* 2004, 2013; Dranow *et al.* 2016), and the sections were photographed on a Zeiss Axio Observer A1 inverted microscope (Leica).

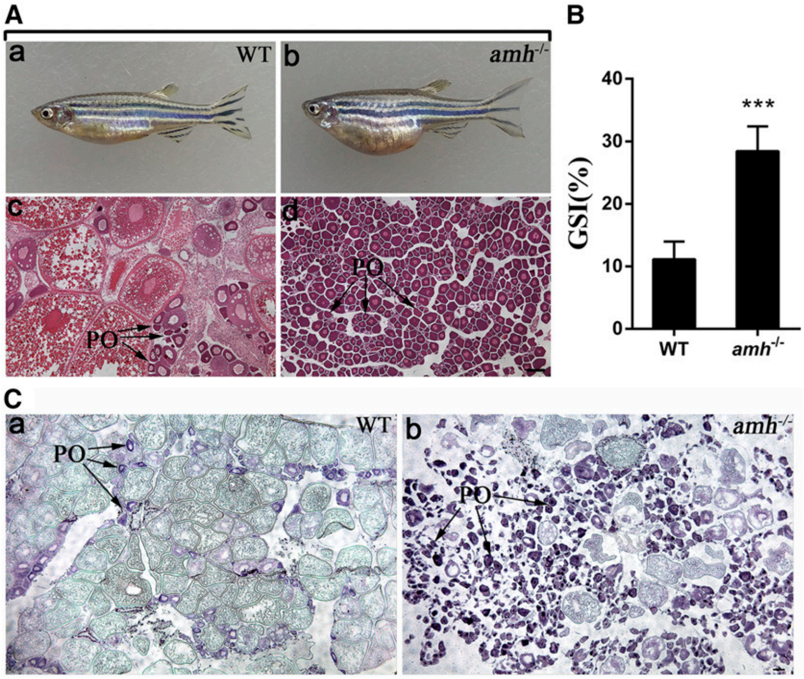

Figure 2 *Amh* mutant females develop hypertrophic ovaries because of overproliferation and differentiation damage of premeiotic oogonia. (A) Gross morphology (a and b) and ovary histological examination (c and d) of WT female and *amh* mutant at 6 months old. (B) GSI changes of WT and *amh* mutant females at 5 months old (mean ± SD, $n = 4$). (C) *nanos2* RNA *in situ* hybridization of WT (a) and *amh* mutant (b) ovaries at 4 months old. Premeiotic oogonia (PO) are marked by arrows. Bar, 100 μm. *** $P <$ 0.001.

RNA isolation and quantitative real-time PCR

Testis RNA isolation and quantitative real-time PCR (qPCR) analysis were performed to evaluate the expression changes of sex-associated genes, between WT and the corresponding mutant testes at different stages. Total RNA samples were isolated from zebrafish testes at different stages (WT and *amh* mutant testes at 180 days postfertilization (dpf); WT and *dmrt1* mutant testes at 27, 33, 43, 54, 75, and 180 dpf) using the SV Total RNA Isolation System (Promega, Madison, WI). The isolated RNAs were respectively reverse transcribed with the GoScript Reverse Transcription System (Promega) according to the manufacturer's instruction. Then, qPCR reactions were performed on the CFX96 Touch Real-Time PCR Detection System (Bio-Rad, Hercules, CA) using iQ SYBR Green Supermix (Bio-Rad) as previously described (Neumann *et al.* 2011). Elongation factor 1α (ef1α) was used as the endogenous control.

The selected sex-associated genes included germ cell markers, *vasa* (Yoon *et al.* 1997), *dnd* (Weidinger *et al.* 2003), *piwil1* expressed in all generations of type A spermatogonia (Chen *et al.* 2013), *dazl* mainly expressed in type B spermatogonia (Chen *et al.* 2013), *plzf* expressed in both type A and B spermatogonia (Ozaki *et al.* 2011), *nanos2* expressed in premeiotic spermatogonia (Beer and Draper 2013), and *sycp3* expressed only in spermatocytes (Ozaki *et al.* 2011). The Sertoli cell-related genes are *amh*, *sox9a* (Rodríguez-Marí *et al.* 2005; Skaar *et al.* 2011), *dmrt1* (Webster *et al.* 2017), *gsdf* (Gautier *et al.* 2011), and *ar* (de Waal *et al.* 2008). The steroidogenic genes expressed in Leydig cells are *star*, *hsd3b*, *cyp11b*, and *cyp17a1* (Wang and Orban 2007; Arukwe 2008; Hinfray *et al.* 2011; Baudiffier *et al.* 2012). Each experiment was analyzed in triplicate and the data were analyzed using the $2^{-\Delta\Delta Ct}$ program. Primer sequences are shown in Table S1 in File S1.

Analysis of apoptosis

Apoptosis in WT and mutant testes was detected by TUNEL using the In-Situ Cell Death Detection Kit, Fluorescein (Roche) according to the manufacturer's instructions. TUNEL and specific antibody double labeling was performed as described (Sweeney *et al.* 2012). The slides were photographed on a Leica SP8 confocal microscope and the number of apoptotic cells on each section was counted as described (Mei *et al.* 2008).

Statistical analysis

All experiments were performed at least in triplicate. More than three animals were analyzed in each experimental group. The data were shown as mean ± SD, and $P < 0.05$ was considered statistically significant after using Student's *t*-test to identify statistical differences between the groups. Statistical analysis was performed with SPSS software and graphs were plotted using GraphPad Prism 6 (La Jolla, CA).

Data availability

Strains used are available upon request. File S1 contain the Figures S1–S7 and Table S1. All primers used in this study are listed in Table S1 in File S1.

Results

Generation and characterization of amh-mutated zebrafish

Zebrafish *amh* encodes a protein with 549 amino acids, containing TGF-β domain at the C terminus and AMH domain in the middle. To investigate the function of *amh*, CRISPR/Cas9 was performed to generate *amh*-mutated zebrafish. The targeting site was chosen in the sixth exon to disrupt both the

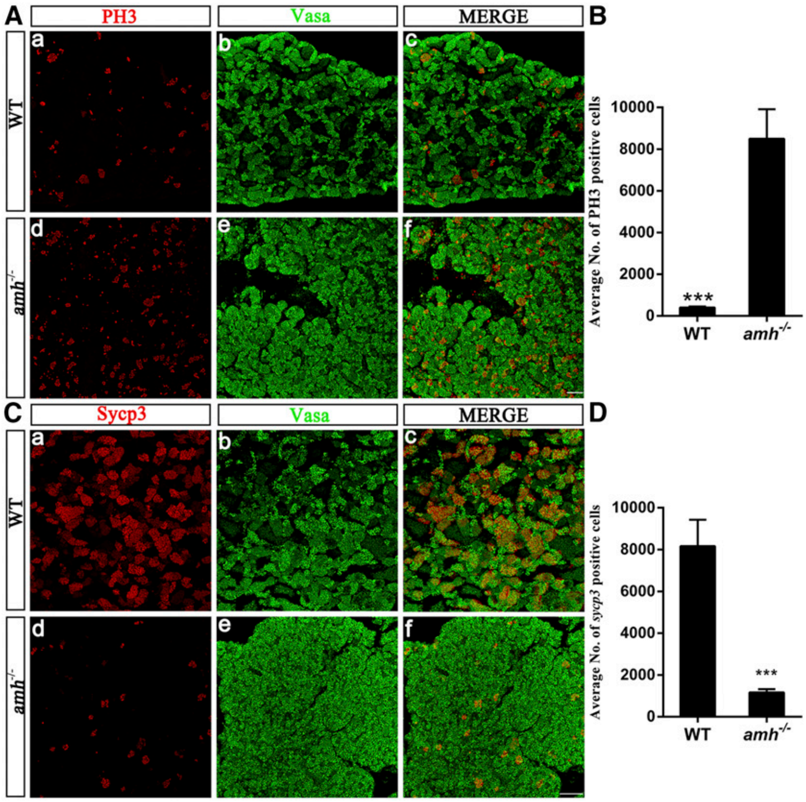

Figure 3 *Amh* deficiency causes overproliferation and differentiation damage of male germ cells. (A) Immunofluorescence staining of WT (a–c) and *amh* mutant (d–f) testis sections at 6 months old with PH3 antibody (a) and Vasa antibody (b), respectively. c is the merge of a and b. (B) Quantification of average PH3-positive cell numbers per section in WT and *amh* mutants (mean ± SD, n = 3). (C) Immunofluorescence staining of WT (a–c) and *amh* mutant (d–f) testis sections at 6 months old with Sycp3 antibody (a) and Vasa antibody (b), respectively. c is the merge of a and b. (D) Quantification of average Sycp3-positive cell numbers per section in WT and *amh* mutants (mean ± SD, n = 3). Bar, 75 μm. *** $P < 0.001$.

AMH domain and TGF-β domain. The sequencing results showed that several types of mutations have passed through the germline (data not shown). Finally, 5-bp deletions (named *amh*Δ5) and 17-bp insertions (named *amh*+17) were identified and chosen to establish mutant lines (Figure S1A in File S1). The genotypes of WT and two homozygotes were confirmed by genomic sequencing (Figure S1B in File S1). The mutations in *amh*Δ5 and *amh*+17 resulted in the ORF shift and caused premature termination codons. Both mutants lost the AMH domain and TGF-β domain (Figure S1C in File S1).

Loss of *amh* function caused the dysregulation of sexual development. We found all homozygous *amh* mutant fish displayed female-biased sex ratios. The percentage of females was ~71% (46 females and 19 males) in the homozygotes, whereas the percentages of females were 46% (51 females and 59 males) in the heterozygotes and 40% (22 females and 33 males) in WT (Figure S2 in File S1). The observed genotype distribution among the progenies was as expected (χ^2 = 0.545, n = 230, P = 0.761), and the observed sex distribution of homozygotes was significantly different from that of heterozygotes ($\chi^2 = 8.887, n = 175, P = 0.003$) or WT ($\chi^2 = 10.267$, $n = 120, P = 0.001$). Thus, we confirm that *amh* is required for normal sex ratios in zebrafish.

Loss of amh function causes dysregulation of germ cell development

At 2.5 months of age, *amh* mutant males had the normal body shape of WT, but an enlarged abdomen was observed at 4 and 6 months of age (Figure 1A). WT zebrafish males exhibited normal secondary sex characteristics, including slender body, darker yellow pigmentation, and presence of breeding tubercles (Dranow *et al.* 2013). However, the yellow fin pigmentation was significantly reduced in *amh*-mutated males (Figure 1A). WT zebrafish testes almost achieved a maximum size at 2.5 months old. In contrast, *amh* mutant testes were found to continue growing after sexual maturity (Figure 1B). *Amh* mutant males had normal reproductive capacity at 2.5 months old, even though the GSI (gonadosomatic index) was slightly increased. However, the homozygous mutated males gradually lost reproductive capacity by 3 months of age (Figure 1C). After dissection, we observed that abdomens of *amh* mutants were occupied by hypertrophic testes, while the other internal organs were squeezed (Figure 1, D and E). To identify the testicular structure defects in *amh* mutants, we analyzed the histology of hypertrophic testes with H&E and immunofluorescent staining. At 6 months of age, WT testes exhibited normal testicular structure, consisting of spermatogenic cysts with spermatogonia, spermatocytes, spermatids, and mature spermatozoa. And, successive differentiation stages of germ cells were observed (Figure 1F). In contrast, abnormal structures were detected in the hypertrophic testes, in which numerous spermatogonium-like cells were filled, whereas only a few spermatids and spermatozoa were seen (Figure 1, G and H). Anti-Vasa immunofluorescence localization indicated that the hypertrophic testes in *amh* mutants were filled with much more Vasa-positive germ cells and fewer spermatids and spermatozoa (Figure 1, J and K) than the control testes (Figure 1I).

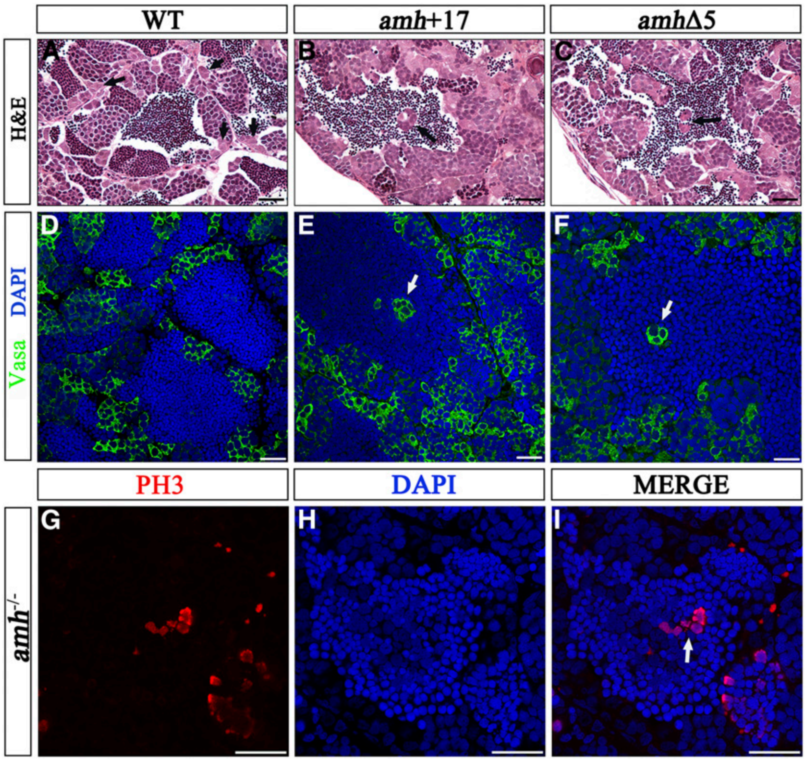

Figure 4 *Amh* mutant testes produce a number of ectopic spermatogonium-like cells. (A–C) H&E staining of testis sections from WT, *amh*+17, and *amh*Δ5 zebrafish at 3 months old. (D–F) Immunofluorescence staining of WT, *amh*+17, and *amh*Δ5 testis sections with anti-Vasa antibody and DAPI at 3 months old. (G–I) Immunofluorescence staining of mutant testis sections with PH3 antibody and DAPI at 3 months old. I is the merge of G and H. Spermatogonia in WT and ectopic spermatogonium-like cells in *amh* mutants are marked by arrows. Bar, 25 μm.

Phenotypes and gonadal tissues of *amh*-mutated females were also investigated. Homozygous females had similar phenotypes to homozygous males, including enlarged abdomen and hypertrophic ovary (Figure 2A). At 6 months of age, WT ovaries showed all stages of oocyte maturation from primary growth oocyte to mature oocyte. In contrast, the hypertrophic ovaries of homozygous females were filled with lots of primary growth oocytes and the oocyte maturation was arrested at an early stage, indicating that loss of *amh* function resulted in an excessive proliferation of germ cells and a profound oocyte maturation defect (Figure 2A). And, the homozygous females had a significant increase in GSI compared with the control (Figure 2B). We further confirmed that these accumulated germ cells are premeiotic oogonia by RNA *in situ* hybridization with a premeiotic germ cell marker *nanos2* (Beer and Draper 2013) at 4 months of age (Figure 2C, a and b). Taken together, *amh* deficiency causes overproliferation and impaired differentiation of germ cells. Thus, *amh* is essential for regulating germ cell differentiation in both male and female zebrafish.

We further checked the cell proliferation by immunofluorescence with PH3 antibody, a mitosis marker for cell proliferation, in both WT and *amh* mutant testes. Two adjacent sections (4 μm) were immunohistologically stained with PH3 and Vasa antibody, respectively. As expected, there was a large increase in the number of PH3-positive cells in *amh*-deficient testes (Figure 3A). Almost all of the PH3-positive cells were Vasa-positive in *amh* mutants (Figure 3A, d–f). Statistical analysis showed that the average number of PH3-positive cells per section in *amh* mutants (mean = 8496, n = 3) was ~21-fold higher than in WT (mean = 400, n = 3), suggesting that the germ cells might have an excessive proliferation (Figure 3B). Then we examined the state of germ cell differentiation in the *amh*-mutated testes by immunohistological staining with antibody of Sycp3, a meiosis marker expressed in spermatocytes. Two adjacent sections (4 μm) were stained with Sycp3 and Vasa, respectively (Figure 3C). The results showed that Sycp3-positive cells were enriched in the WT testes, and most Vasa-positive cells were Sycp3-positive (Figure 3C, a–c). By contrast, in *amh*-deficient testes, the germ cells lacked or had very low levels of Sycp3 expression, and only a few Vasa-positive cells were Sycp3-positive (Figure 3C, d–f), suggesting that the accumulated germ cells should be premeiotic germ cells. Statistical analysis indicated that the average number of both Sycp3- and Vasa-positive cells per section in WT (mean = 8167, n = 3) was ~7-fold higher than in *amh* mutants (mean = 1166, n = 3) (Figure 3D), revealing a severely impaired differentiation of male germ cells.

Histologic analysis of testes was performed at 3 months of age when *amh* mutants began to lose the reproductive capacity. In WT males, successive spermatogenic cells, including spermatogonia, spermatocytes, spermatids, and spermatozoa (from the edge to the center of lobules) were evident, and small clusters of spermatogonia (arrows) were observed to locate on the testicular lobule edge (Figure 4A), whereas in both *amh*Δ5 and *amh*+17 mutated testes, ectopic clusters of spermatogonium-like cells (arrows) were detected among the spermatozoa (Figure 4, B and C). Moreover, these ectopic spermatogonium-like cells among the spermatozoa were

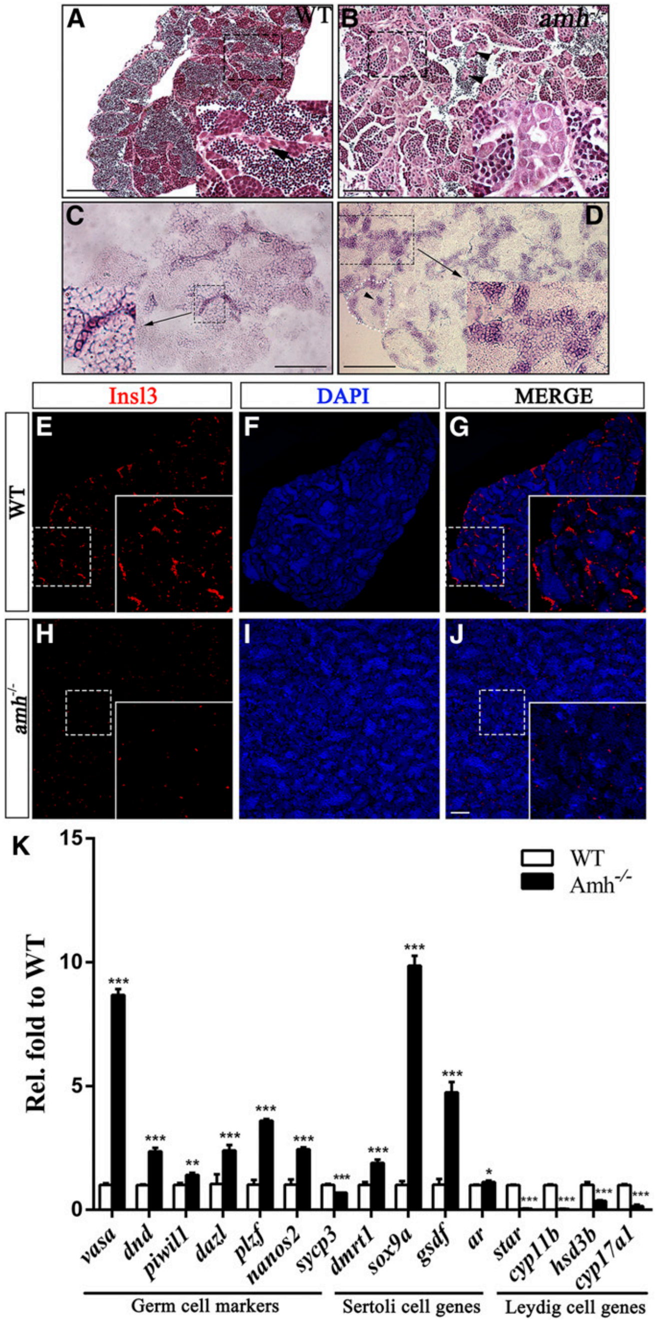

Figure 5 *Amh* deficiency causes dysregulation of male germ cell differentiation-related genes and gonadal somatic cell development-related genes. (A and B) H&E staining of WT testis (A) and *amh* mutant testis (B) at 2 months old. (C and D) *In situ* hybridization for spermatogonium-specific marker *nanos2* in WT testis (C) and *amh* mutant testis (D) at 2 months old. (E–J) Immunofluorescence staining of WT (E–G) and *amh* mutant (H–J) testis sections with Insl3 antibody at 6 months old. (K) Expression changes of male germ cell differentiation-related genes and gonadal somatic cell development-related genes in *amh* mutant testes at 6 months old. Spermatogonia in WT are marked by arrows and ectopic clusters of spermatogonia in *amh* mutants are marked by arrowheads. Bar, 100 μm. * $P < 0.05$, ** $P < 0.01$, *** $P < 0.001$.

confirmed as Vasa-positive (Figure 4, D–F) and PH3-positive (Figure 4, G–I). These data indicate that *amh* function loss causes dysregulation of germ cell development and lead to the overproliferation of spermatogonia in *amh*-mutated testes.

Abnormal expression changes of male germ cell differentiation-related genes and gonadal somatic cell development-related genes in amh mutant testes

Although *amh* mutant males had normal reproductive capacity at ~2.5 months of age, histologic analysis of testes observed the number increase and cluster formation of spermatogonia (arrows) at 2 months of age (Figure 5, A and B). And, the result was confirmed by significantly increasing expression signal of *nanos2*, a marker enriched in zebrafish spermatogonia. Compared with the WT control (Figure 5C), ectopic clusters of *nanos2* mRNA expression (arrowhead) were detected within the lobules (Figure 5D). *Insl3* is a somatic Leydig cell marker and stimulates spermatogonial differentiation in adult zebrafish testes (Good-Avila *et al.* 2009; Assis *et al.* 2016). We further checked the expression of *Insl3* by immunohistochemical staining. In WT testes, many clusters of Leydig cells were present in the interstitial area (Figure 5, E–G), whereas only a few single Leydig cells among the disorganized germ cells were detected in *amh* mutants (Figure 5, H–J), suggesting that Leydig cell differentiation failed in *amh*-deficient testes.

Moreover, we investigated the expression changes of several male germ cell differentiation-related genes and gonadal somatic cell development-related genes in *amh* mutant testes by qPCR at 6 months of age (Figure 5K). In seven germ cell marker genes, six spermatogonium marker genes, namely, *vasa*, *dnd*, *piwil1*, *dazl*, *plzf*, and *nanos2*, were significantly up-regulated, whereas meiosis marker gene *sycp3*, only expressing in spermatocytes, was downregulated in the *amh*-mutated testes (Figure 5K, left). These results were consistent with our histological observation that spermatogonia had excessive proliferation and spermatogenic cell differentiation was severely impaired. Four Sertoli cell marker genes, including *dmrt1*, *sox9a*, *gsdf*, and *ar*, were significantly upregulated in *amh*-mutated testes. However, four Leydig cell marker genes, namely, *star*, *hsd3b*, *cyp11b*, and *cyp17a1*, were significantly downregulated, suggesting that *amh* might be required for androgen synthesis because of their association with steroidogenesis. These data suggest that *amh* should play crucial roles in germ cell differentiation and spermatogenesis because loss of *amh* function leads to abnormal expression changes of male germ cell differentiation-related genes and gonadal somatic cell development-related genes.

Generation and characterization of dmrt1-mutated zebrafish

To investigate the functions of *dmrt1* in zebrafish germ cell development, the CRISPR/Cas9 system was used to generate *dmrt1*-mutated zebrafish. The targeting site was chosen in the first exon and closed to the start codon. Finally, 14-bp deletions (named *dmrt1*Δ14) and 11-bp insertions (16-bp insertions plus 5-bp deletions, named *dmrt1*+11) were identified and chosen to establish mutant lines (Figure S3A in File

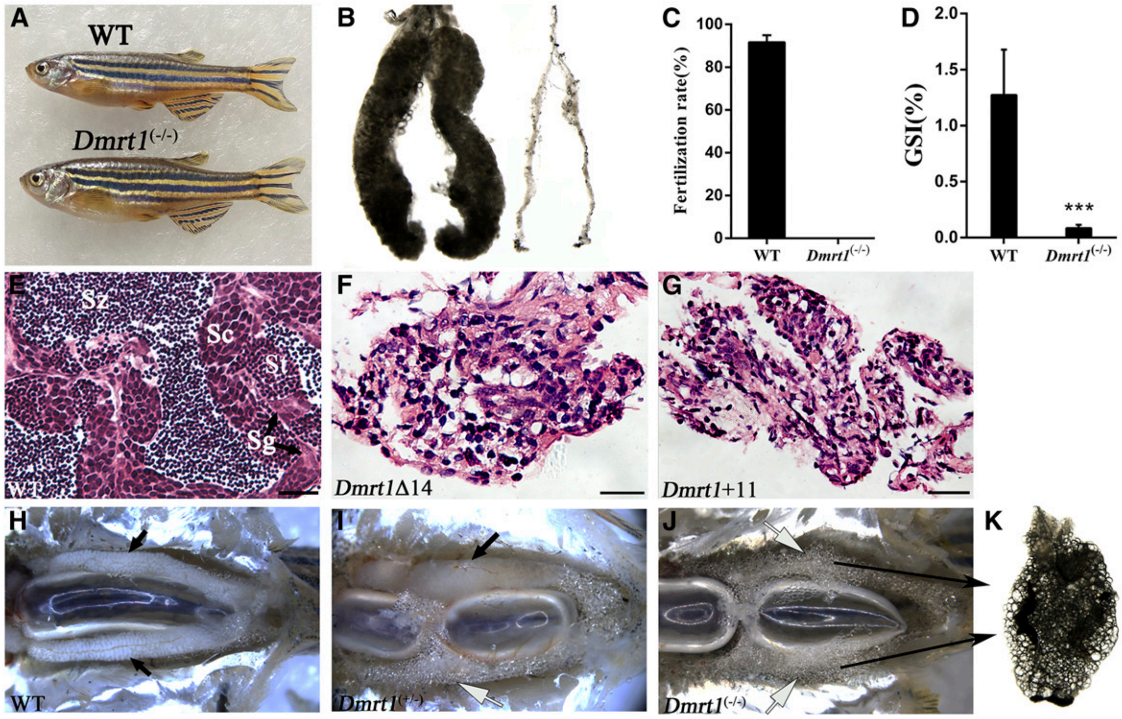

Figure 6 Phenotypic and testis tissue analysis of *dmrt1* mutants. (A) Gross morphology comparisons between WT and *dmrt1* mutant males. (B) Anatomical observation of WT (left) and *dmrt1* mutant (right) testes at 75 dpf. (C) Fertilization rate difference of WT and *dmrt1* mutant males by crossing with WT females at 90 dpf (mean ± SD, n = 8). (D) GSI difference of WT and *dmrt1* mutant males at 75 dpf (mean ± SD, n = 7). (E–G) Histological observation of testes from WT (E), *dmrt1*Δ14 (F), and *dmrt1*+11 (G) by H&E staining at 90 dpf. (H–K) Anatomical observation of testes in WT, heterozygotes (*dmrt1*$^{+/-}$), and homozygotes (*dmrt1*$^{-/-}$) at 240 dpf. Testes are marked by black arrows and adipose tissue associated with testes is marked by white arrows. Sg, spermatogonia; Sc, spermatocytes; St, spermatids; Sz, spermatozoa. Bar, 20 μm. *** $P < 0.001$.

S1). The genotypes of WT and two kinds of homozygotes were confirmed by genomic sequencing (Figure S3B in File S1). The mutations in *dmrt1*Δ14 and *dmrt1*+11 resulted in the ORF shift and caused premature termination codons (Figure S3C in File S1).

The *dmrt1* mutants displayed female-biased sex ratios, because the percentages of females were ∼47 and 79% in the heterozygotes and homozygotes, respectively (Figure S4 in File S1). The observed genotype distribution among the progenies was as expected ($\chi^2 = 0.020$; $n = 102$; $P = 0.889$) and the observed sex distribution of homozygotes was significantly different from that of heterozygotes ($\chi^2 = 10.141$; $n = 102$; $P = 0.001$). We found that the homozygous *dmrt1* mutant females were fertile and exhibited the same normal ovarian development as WT females (Figure S5 in File S1). Significantly, both the *dmrt1*Δ14 and *dmrt1*+11 mutant males were viable (Figure 6A), but thin thread-like testicular structures were observed in the mutated adults compared with typical testes in the control (Figure 6B). And, all the *dmrt1*-mutated males were infertile (Figure 6C). We also found a significant GSI decrease in homozygous mutants compared with WT (Figure 6D). Compared with normal testicular architecture (Figure 6E) in WT control adults, both the *dmrt1*Δ14 and *dmrt1*+11 mutant testes showed severe histological abnormalities, including some disorganized fibroblast-like somatic cells and diffused vacuolation in the severely hypoplastic testes (Figure 6, F and G). At 8 months old, the WT testes still had two normal lobes (Figure 6H); however, ∼50% heterozygous males displayed partially regressed testis lobes relative to WT (Figure 6I), and all homozygous testes had severely regressed lobes with a mass of adipose tissue (Figure 6, J and K). In addition, H&E staining showed a large number of disorganized fibroblast-like somatic cells in the regressed testes (Figure S6 in File S1).

Dmrt1 deletion impairs male germ cell development and testicular lobule formation

Subsequently, we investigated the detailed defects of *dmrt1* deletion during testis development and spermatogenesis. At 28 dpf, WT testes showed abundant Vasa-positive male germ cells, including different stages of spermatogonia (sg) (Figure 7, A and B), whereas *dmrt1*-mutated testes displayed fewer spermatogonia and residual primary oocytes (po) (Figure 7, C and D). At 34 dpf, testicular lobules with spermatogonia, spermatocytes (sc) and spermatids (st) appeared in WT testes (Figure 7, E and F). Male germ cells were significantly reduced in *dmrt1*-mutated testes, and the degenerated oocytes (do) still existed, indicating that morphological alteration from ovarian follicle to testis cord failed (Figure 7, G and H). At 43 and 54 dpf, WT testes showed typical testicular structure, including well-organized spermatogonia, spermatocytes, and spermatids (Figure 7, I, J, M, and N).

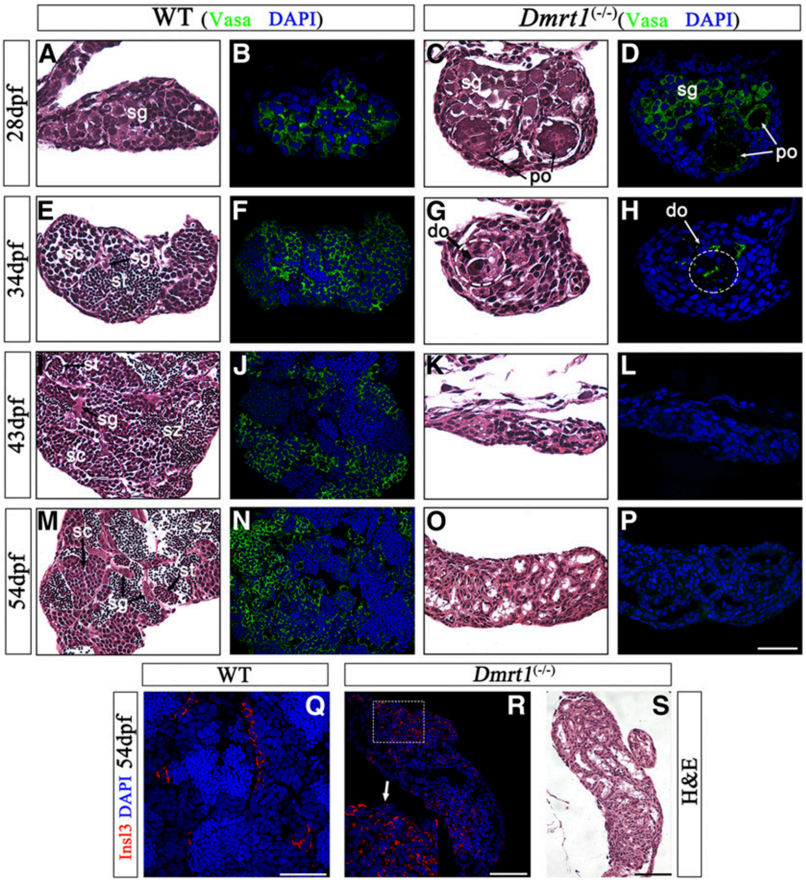

Figure 7 *Dmrt1* is required for male germ cell development and testicular lobule formation. (A–P) Histological observation of WT and *dmrt1* mutant testes at 28 dpf (A–D), 34 dpf (E–H), 43 dpf (I–L), and 54 dpf (M–P) by H&E staining (A, C, E, G, I, K, M, and O) and Vasa antibody immunofluorescence staining (B, D, F, H, J, L, N, and P) of WT and *dmrt1* mutant testes. (Q and R) Immunofluorescence staining of WT (Q) and *dmrt1* mutant (R) testis sections with anti-Insl3 antibody at 54 dpf. (S) H&E staining of *dmrt1* mutant testis at 54 dpf. Numbers of animals in each experimental group: $n = 4$. Sg, spermatogonia; Sc, spermatocytes; St, spermatids; Sz, spermatozoa; Po, primary oocytes; Do, degenerated oocytes. Bar, 25 μm.

However, mutant testes were completely devoid of normal testicular structure and lost all Vasa-positive germ cells, with only disorganized somatic cells (Figure 7, K, L, O, and P). Compared with WT testes, there was an apparent increase in the number of Leydig cells in the mutant testes, as revealed by immunofluorescent staining with antibody of Insl3, a marker of Leydig cell (Figure 7, Q and R). These results indicate that *dmrt1* deletion impairs male germ cell development and testicular lobule formation.

Dmrt1 is required for proliferation and maintenance of male germ cells

To better understand the effects of *dmrt1* deficiency on testis development, we first performed immunofluorescent staining with PH3 antibody, a mitosis marker for cell proliferation. At 28 dpf, PH3-positive proliferating cells were enriched in the WT testes (Figure 8A, a and b). In contrast, few PH3-positive cells were detected in the *dmrt1* mutant testes (Figure 8A, c and d). At 33 and 53 dpf, the depletion of PH3-positive proliferating cells was observed in the *dmrt1* mutants (Figure 8A, g, h, k, and l), compared to a number of positive proliferating cells in the WT testes (Figure 8A, e, f, i, and j). Statistical analysis indicated that the average number of PH3-positive cells in WT (mean = 47.14, $n = 7$) was ~64-fold higher than in *dmrt1* mutants (mean = 0.73, $n = 11$) at 33 dpf, revealing a significant decrease of proliferating cells in the *dmrt1* mutant testes (Figure 8B).

The development of male germ cells was further examined by immunohistological staining with antibody of Sycp3, a meiotic marker of germ cell. At 18 dpf, we did not observe any Sycp3-positive cells in the bipotential gonads of both WT and mutant zebrafish (Figure 8C, a–d). However, at 26 dpf, the number of observed Sycp3-positive cells was less in *dmrt1*-mutated testes compared with the control (Figure 8C, e–h). At 30 dpf, male germ cells were significantly reduced in *dmrt1*-mutated testes as we only detected a few of Sycp3-positive cells. In contrast, WT testes exhibited more signals of Sycp3 (Figure 8C, i–l). At 40 dpf, although Sycp3-positive cells were enriched in the WT testes, we did not find any Sycp3 signals (Figure 8C, m–p). Thus, the gradual loss of Sycp3 expression in mutant testes supported the idea that *dmrt1* is essential for normal development of male germ cell in zebrafish testes (Webster *et al.* 2017).

The apoptosis of male germ cells and somatic cells were evaluated by fluorescent TUNEL analysis. At 27 and 31 dpf, compared to the sporadic signals in the testes of WT control (Figure 9A, a, b, e, and f), we found that the number of TUNEL-positive cells was significantly increased in *dmrt1*-mutated testes (Figure 9A, c, d, g, and h), in spite of the reduced mRNA expression of *p53* (Figure S7 in File S1). Quantification of TUNEL-positive cells in testis sections showed that the average number of apoptotic cells in *dmrt1* mutant testes (mean = 26.13, $n = 8$) was about four-fold higher than in WT (mean = 6.8, $n = 5$) at 31 dpf, suggesting

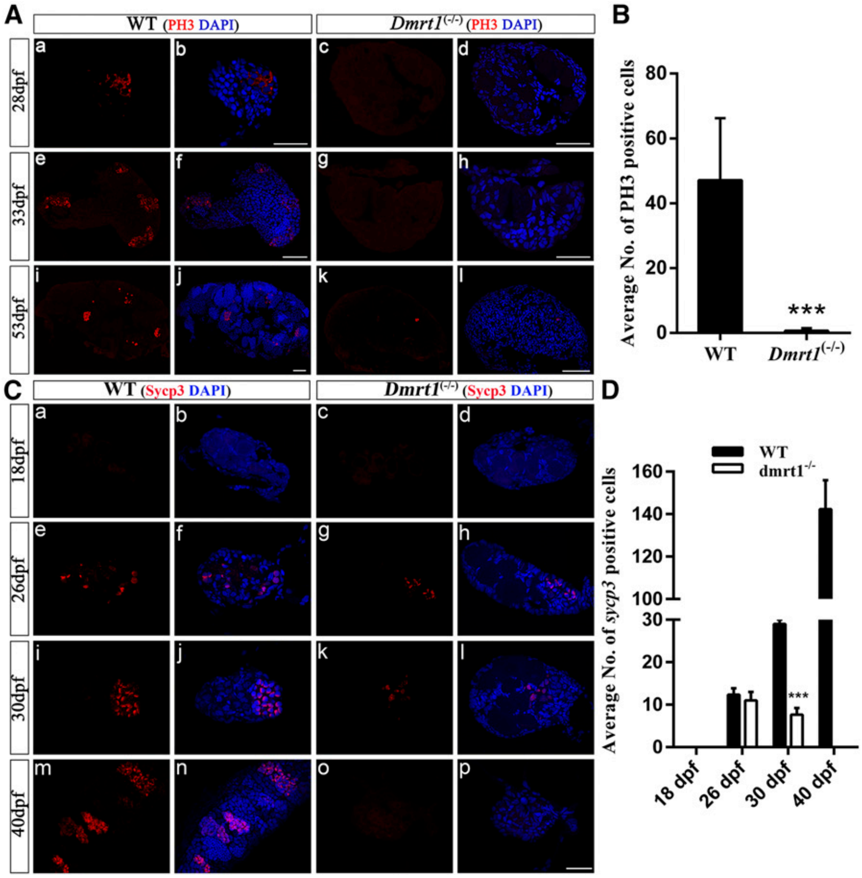

Figure 8 Defective cell proliferation and abnormal male germ cell development in *dmrt1* mutant testes. (A) Immunofluorescence staining of WT and *dmrt1* mutant testis sections with PH3 antibody and DAPI at 28 dpf (a–d), 33 dpf (e–h), and 53 dpf (i–l). (B) Quantified results of average PH3-positive cell numbers per section in WT and *dmrt1* mutant testes at 33 dpf (mean ± SD, numbers of animals used: WT = 7 and mutant = 11). (C) Immunofluorescence staining of WT and *dmrt1* mutant testes with Sycp3 antibody and DAPI at 18 dpf (a–d), 26 dpf (e–h), 30 dpf (i–l), and 40 dpf (m–p). (D) Quantified results of average Sycp3-positive cell numbers per section in WT and *dmrt1* mutants at 18, 26, 30, and 40 dpf (mean ± SD, n = 3). Bar, 25 μm. *** $P < 0.001$.

an abnormal increase of cell apoptosis in *dmrt1* mutant testes (Figure 9B). To determine the type of apoptotic cells, we co-stained Vasa-positive cells by antibody immunofluorescence and apoptotic cells by TUNEL in both WT and *dmrt1* mutant testes at 28 dpf. Almost no apoptotic signals were detected in the germ cells of control testes (Figure 9C, a–c), but a large number of germ cells were found to be co-labeled with Vasa and TUNEL signals within *dmrt1* mutant testes (Figure 9C, d–f), indicating that *dmrt1* is required for the maintenance of early male germ cells. In addition, some TUNEL-positive cells were not observed to be Vasa-positive, implying apoptosis occurrence of some somatic cells (Figure 9C, d–f). Thereby, we further checked the status of somatic cells by double staining with anti-Insl3 (Leydig cell marker) antibody and TUNEL. Many more TUNEL-positive cells were found in *dmrt1*-deficient testes compared with the control at 27 dpf, but none of them was Insl3-positive, suggesting that these apoptotic cells were germ cells and other somatic cells such as Sertoli cells in mutant testes (Figure 9C, a–d). At 54 dpf, when mutant testes were completely devoid of germ cells, only a few TUNEL-positive cells were detected in both mutant and WT testes, and they were not Insl3-positive (Figure 9C, e–h), whereas a large number of Insl3-positive Leydig cells did not undergo apoptosis in *dmrt1*-deficient testes. Therefore, these results indicate that *dmrt1* is specifically required for proliferation and maintenance of male germ cells.

Loss of dmrt1 leads to dysregulation of germ cell-related genes and gonadal somatic cell-related genes

To demonstrate that *dmrt1* plays a key role in both germ line and somatic cell development of zebrafish testes, the expression changes of some germ cell-related genes and gonadal somatic cell-related genes were evaluated by qPCR between WT and the corresponding *dmrt1*-mutated testes during gonad development (Figure 10). At 27 dpf, the germ cell marker genes, including *vasa*, *piwil1*, *dnd*, and *sycp3*, were upregulated, whereas *dazl* was downregulated in *dmrt1*-mutated testes, compared with WT control. However, at 33 dpf, the expression of all germ cell marker genes was significantly reduced, except that *dnd* was slightly upregulated in *dmrt1*-mutated testes. At the later stages of testis development, including 43, 54, and 75 dpf, there was almost no transcript expression of these five germ cell marker genes in *dmrt1*-mutated testes (Figure 10, A–E). Next, we checked the expression dynamics of four Sertoli cell-related genes. *Sox9a*, *gsdf*, and *ar* were first upregulated at 27 dpf, then gradually downregulated at 33, 43, and 54 dpf. Finally, *sox9a* disappeared at 54 dpf and *gsdf* disappeared at 75 dpf. Strikingly, the expression of *amh* was absent at all stages (Figure 10, F–I). Further, we analyzed expression changes of two key steroidogenic genes *hsd3b* and *cyp17a1* that were proposed to express in Leydig cells (Figure 10, J and K). Their dynamic expression did not show a relatively consistent trend, while

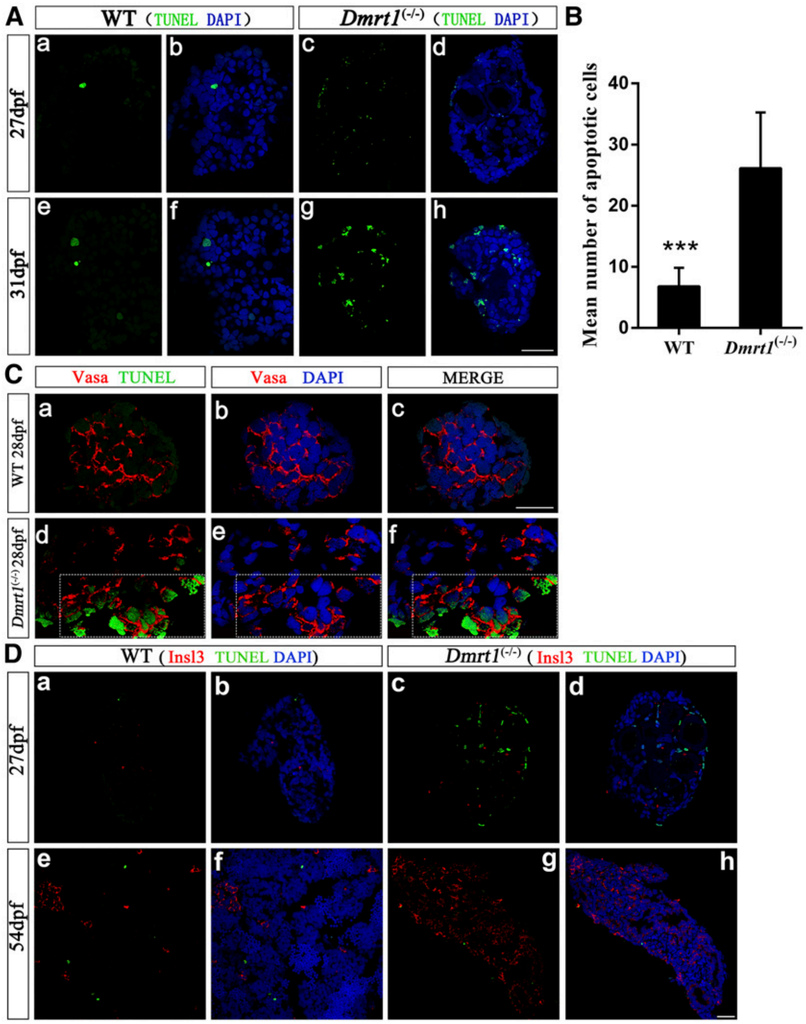

Figure 9 Apoptosis is induced in the *dmrt1* mutant testes. (A) TUNEL and DAPI staining in testis sections of WT and *dmrt1* mutants at 27 dpf (a–d) and 31 dpf (e–h). (B) Quantified results of average number of apoptotic cells assessed by TUNEL in WT and *dmrt1* mutants at 31 dpf (mean ± SD, numbers of animals used: WT = 5 and mutant = 8). (C) Double immunofluorescence staining for TUNEL (in green) and germ cell marker Vasa antibody (in red) in WT and *dmrt1* mutants at 28 dpf. (D) Triple fluorescence staining with anti-Insl3 antibody, TUNEL, and DAPI in WT and *dmrt1* mutant testes at 27 dpf (a–d) and 54 dpf (e–h). Bar, 25 μm. *** $P < 0.001$.

cyp17a1 expression displayed an increasing trend in the *dmrt1*-mutated testes compared to the control, especially at later stages. Moreover, we constructed a graphical heat map to show the expression changes of all 11 investigated genes during testis development when the function of *dmrt1* was lost (Figure 10L). Our data indicated that a compensation effect might be activated at early stages, such as 27 dpf in all cell lineages of the *dmrt1*-mutated testes, but the expression changes of three kinds of genes were consistent with our histological results that germ cells and Sertoli cells were absent or impaired (Figure 7), whereas numerous Insl3-positive Leydig cells existed in residual testes of the *dmrt1* mutants (Figure 9). Therefore, their expression changes suggest that *dmrt1* should be required for the maintenance of both germline genes and Sertoli cell genes during testis development.

Discussion

Germ cells have been extensively studied in recent years, because they provide the genetic linkage between generations in multicellular organisms (Xu *et al.* 2010; Gui and Zhu 2012). Here we investigated the roles of *amh* and *dmrt1* in zebrafish germ cell development by CRISPR/Cas9 technology. All the male and female *amh* mutants developed hypertrophic gonads. *Amh*-mutated males showed hypertrophic testes with excess proliferation of Vasa-positive spermatogonium-like cells within the lobules. Moreover, the hypertrophic testes were filled with disorganized *nanos2*-positive spermatogonia and the number of Sycp3-positive cells was severely reduced, suggesting the uncontrolled proliferation and impaired differentiation of male germ cells. *Dmrt1*-mutated testes displayed a progressive loss of spermatogenesis, in which both germ cell and Sertoli cell marker genes were significantly downregulated or completely inhibited at later stages, whereas Leydig cell marker genes were upregulated (Figure 10), and the increase expression was consistent with immunohistochemical observation by Leydig cell marker Insl3 antibody (Figure 9D). Based on these findings, we propose a hypothesized model in which *amh* and *dmrt1* cooperatively regulate zebrafish male germ cell self-renewal and differentiation. As shown in Figure 11, *dmrt1* is required for the maintenance and self-renewal of early male germ cells, because *dmrt1* mutation impairs male germ cell development and testicular lobule formation and leads to regressed testis, whereas *amh* is decisive for controlling

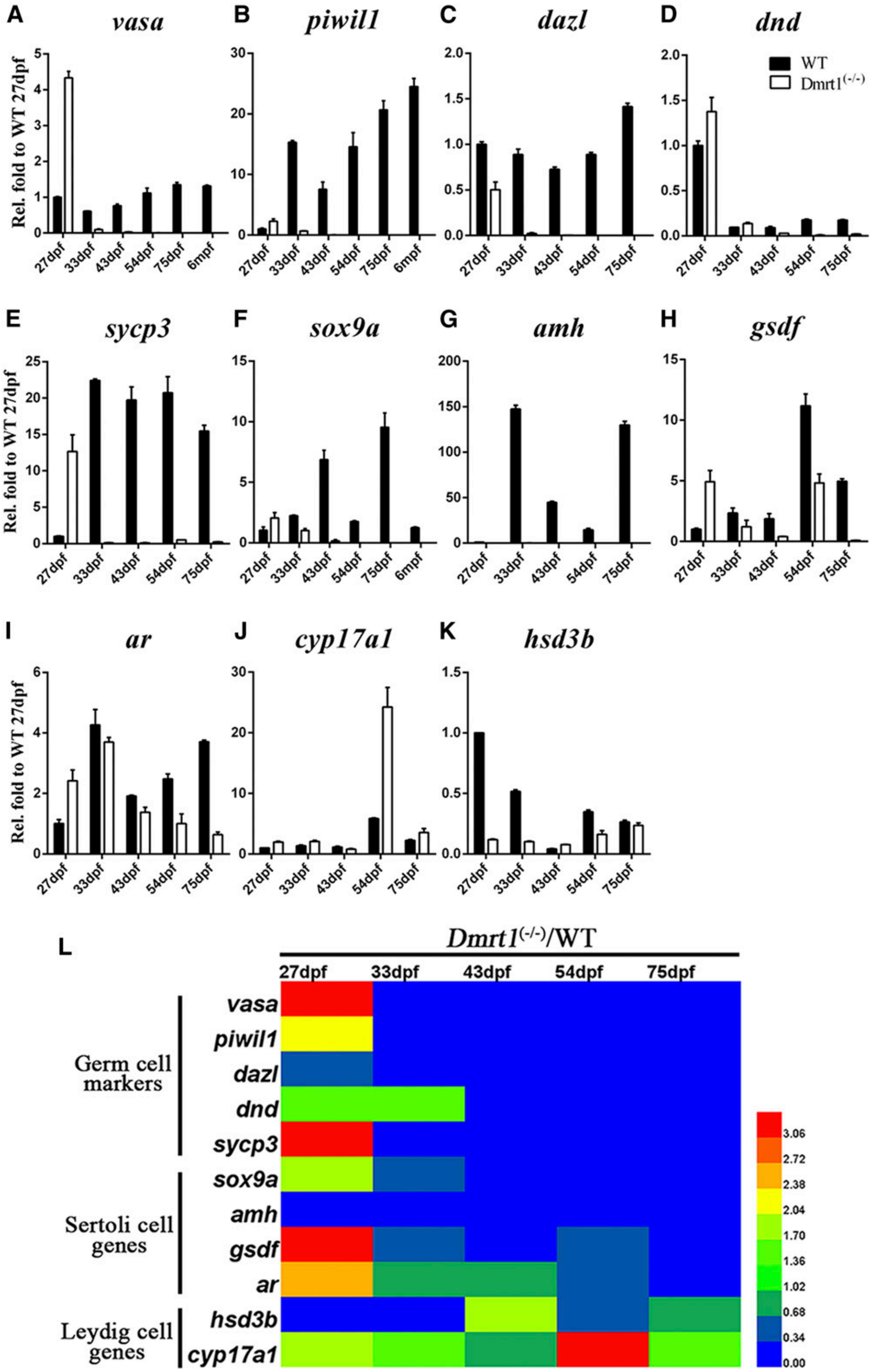

Figure 10 Disruption of *dmrt1* expression causes dysregulation of germ cell-related genes and gonadal somatic cell-related genes. (A–K) qPCR analysis of these genes including *vasa*, *piwil1*, *dazl*, *dnd*, *sycp3*, *sox9a*, *amh*, *gsdf*, *ar*, *cyp17a1*, and *hsd3b*, between WT and the corresponding *dmrt1* mutant testes at 27, 33, 43, 54, and 75 dpf ($n = 3$). (L) Heat map constructed to compare the expression changes of all 11 investigated genes during testis development.

the balance between proliferation and differentiation of male germ cells, because *amh* function loss causes overproliferation and accumulation of spermatogonia and results in hypertrophic testis (Figure 11A). Therefore, *dmrt1* activates *amh* expression, whereas *amh* negatively regulates *dmrt1* expression. Moreover, *dmrt1* maintains self-renewal and proliferation of early male germ cells, while *amh* inhibits excessive proliferation of spermatogonia and maintains normal differentiation. In other words, *amh* and *dmrt1* cooperatively keep the balance of spermatogenesis by regulating self-renewal, proliferation, and differentiation of male germ cells (Figure 11B).

Initially, *amh* was detected in Sertoli cells and responsible for regression of Müllerian ducts in mammals (Kobayashi *et al.* 2011). What are the functions of *amh* orthologs in fish species?

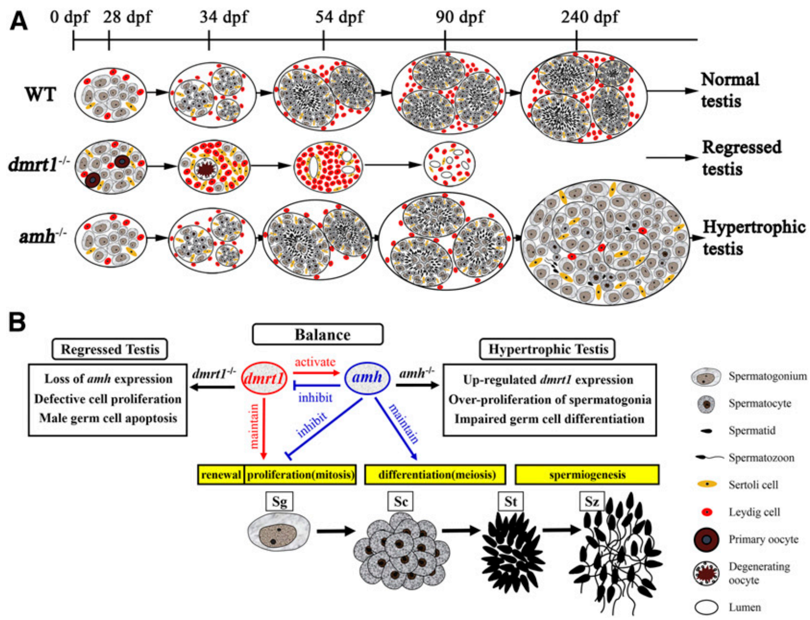

Figure 11 Schematic diagram for the cooperative regulation between *amh* and *dmrt1* in zebrafish male germ cell self-renewal and differentiation. (A) Histological and cytological characteristics of WT, *dmrt1*$^{-/-}$, and *amh*$^{-/-}$ testes at different stages. (B) Detailed diagram about the cooperative interactions and distinct functions of *dmrt1* and *amh* in keeping the balance of spermatogenesis by regulating self-renewal, proliferation, and differentiation of male germ cells. Sg, spermatogonia; Sc, spermatocytes; St, spermatids; Sz, spermatozoa.

In vitro studies indicated that zebrafish Amh production in Sertoli cells was preferentially localized around type A spermatogonia and inhibited the differentiation of male germ cells (Skaar *et al.* 2011). In medaka *hotei* mutants that lack the function of Amh-type II receptor (AmhrII), one-half of the adult XY homozygous fish were sex reversed into females, and the other half displayed hypertrophic testes (Morinaga *et al.* 2007). In the hypertrophic testes of medaka *hotei* mutants, a hyperproliferation of undifferentiated type A spermatogonia was detected in both juvenile and adult stages, but the number of mitotically quiescent germline cells was normal (Morinaga *et al.* 2007; Nakamura *et al.* 2012). So far, the specific receptors for Amh, such as AmhrII, had been found only in a couple of fish species (Rocha *et al.* 2016). However, AmhrI and AmhrII had not been found in the zebrafish genome. Similar to the phenotypes in medaka *hotei* mutants (Morinaga *et al.* 2007), our zebrafish *amh* mutants showed hypertrophic testes (Figure 1) and highly uncontrolled proliferation of premeiotic spermatogonia (Figure 1 and Figure 3), indicating the conserved roles of Amh/Amhr signaling in male germ cell maintenance and differentiation. Particularly, our studies revealed that the germ cells in *amh*-deficient testes lacked or had very low levels of Sycp3 expression (Figure 3, C and D), confirming the deficiency of spermatogonium differentiation. Besides its roles in testis development, the Amh signal was also revealed to regulate female germ cell differentiation in zebrafish ovary, as an overproliferation of premeiotic oogonia was observed in the hypertrophic ovaries of 4-month-old *amh*-deficient females (Figure 2, C and D). Therefore, our current results suggest that *amh* might act as a guardian to regulate differentiation of both male and female germ cells in zebrafish, because its loss of function leads to overproliferation of both premeiotic spermatogonia and oogonia and thereby forms hypertrophic tumor-like testes or ovaries in the *amh*-deficient males or females (Figure 1 and Figure 2).

Different from mammals and most other fish species, the undifferentiated gonads in zebrafish first differentiate as "bipotential juvenile ovaries," and then half of the juvenile ovaries undergo apoptosis and regression and eventually develop into testes during 20–30 dpf (Wang *et al.* 2007; Orban *et al.* 2009). In zebrafish, primary germ cells are required for female sex differentiation, because loss of primary germ cells led to an all-male sexual phenotype in adults (Slanchev *et al.* 2005). Recently, several genes have been revealed to be involved in zebrafish male sex determination and testicular differentiation. Disruption of zebrafish *fancl* and *fancd1* (*brca2*) gene functions caused female-to-male sex reversal by p53-mediated germ cell apoptosis (Rodríguez-Marí *et al.* 2010, 2011). However, *nr0b1* (*DAX1*) mutation in zebrafish resulted in female-to-male sex reversal in a p53-independent manner (Chen *et al.* 2016). Disruption of *foxl2a* and *foxl2b* function led to the sex reversal from females to males (Yang *et al.* 2017). *Dmrt1* and its paralog gene *dmy* are involved in male sex determination and differentiation in medaka. *Dmrt1* mutation resulted in the sex reversal of XY gonads into ovary type (Matsuda *et al.* 2002; Masuyama *et al.* 2012). In this study, the *dmrt1*-mutated zebrafish generated by CRISPR/Cas9 approach also displayed female-biased sex ratios (Figure S4 in File S1) as recently described by Webster *et al.* (2017). In comparison with the recent report that germ cells were still present in adult *dmrt1* mutant males, our current data observed severely regressed testes with only a mass of adipose tissue (Figure 6, J and K) and complete loss of all germ cells at later stages (Figure 7). The phenotypic difference might be the reflection of different genetic backgrounds between the previous TU strain and the AB strain. Additionally, we performed anit-Vasa immunofluorescence localization, and our current results were confirmed by both general H&E staining and anit-Vasa immunofluorescence staining. Therefore, our current data suggest that *dmrt1* should be required for proliferation and maintenance of male germ cells, because *dmrt1* deletion resulted in loss of all male germ cells and destroyed testicular lobule formation (Figure 6 and Figure 7), and the germ cell damage and testicular tissue destruction were confirmed by severe expression suppression of some germ cell-related genes and gonadal somatic cell-related genes at later stages (Figure 10).

Expressed in Sertoli cells and germ cells, mouse *dmrt1* plays a germ cell-autonomous role and a Sertoli cell-non-autonomous role to promote germ cell development (Kim *et al.* 2007; Agbor *et al.* 2013; Zhang *et al.* 2016). In *dmrt1*-mutated zebrafish testes, we detected the reduced expression of *sox9a*, *amh*, and *gsdf*. Therefore, it is concluded that the male germ cell defects in *dmrt1* mutants are due to loss of *dmrt1* function in both of these cell types. Regardless of male germ cell defects in *dmrt1* mutants, our data showed that the expression of two key steroidogenic genes, *hsd3b* and *cyp17a1*, had no obvious change, which is why we could observe the normal secondary sex characteristics, including slender body, yellow fin pigmentation, and breeding tubercle. It has been shown that Sertoli cells can be reprogrammed to other cell types, such as pluripotent stem cells and fetal-like Leydig cells (Sun *et al.* 2014; Zhang *et al.* 2015a). In *dmrt1*-mutated testes, there are more Insl3-positive Leydig-like cells than the control testes. Whether these Leydig-like cells are reprogrammed from other cell types need further studies.

In conclusion, our current data indicate that *dmrt1* positively regulates *amh* expression, whereas *amh* negatively regulates *dmrt1* expression, and thereby forms a negative feedback loop of *amh* and *dmrt1*. Significantly, *dmrt1* mutants were simultaneously found to lead to complete inhibition of *amh* expression in the examined testes (Figure 10, G and L), implying that *dmrt1* mutants might have same phenotypes with double mutants of *dmrt1* and *amh*. Therefore, *amh* and *dmrt1* cooperatively regulate self-renewal and differentiation of male germ cells in zebrafish.

Acknowledgments

This work was supported by the National Natural Science Foundation of China (31672635), the Key Program of Frontier Sciences of the Chinese Academy of Sciences (CAS) (QYZDY-SSW-SMC025), the Strategic Priority Research Program of CAS (XDA08030201), the Autonomous Project of State Key Laboratory of Freshwater Ecology and Biotechnology (2011FBZ22), and the Autonomous Projects of the Institute of Hydrobiology, CAS (Y25A17 and Y45A171301). The funders had no role in study design, data collection and analysis, decision to publish, or preparation of the manuscript. All authors declare that they have no conflict of interest.

Author contributions: J.M. and J.-F.G. designed research; Q.L., Z.L., and X.Z. performed research; Q.L., L.Z., and J.M. analyzed data; and J.M., Q.L., and J.-F.G. wrote the paper.

Literature Cited

Agbor, V. A., S. Tao, N. Lei, and L. L. Heckert, 2013 A Wt1-Dmrt1 transgene restores DMRT1 to sertoli cells of Dmrt1(−/−) testes: a novel model of DMRT1-deficient germ cells. Biol. Reprod. 88: 51.

Arukwe, A., 2008 Steroidogenic acute regulatory (StAR) protein and cholesterol side-chain cleavage (P450scc)-regulated steroidogenesis as an organ-specific molecular and cellular target for endocrine disrupting chemicals in fish. Cell Biol. Toxicol. 24: 527–540.

Assis, L. H., D. Crespo, R. D. Morais, L. R. Franca, J. Bogerd *et al.*, 2016 INSL3 stimulates spermatogonial differentiation in testis of adult zebrafish (*Danio rerio*). Cell Tissue Res. 363: 579–588.

Baudiffier, D., N. Hinfray, M. Vosges, N. Creusot, E. Chadili *et al.*, 2012 A critical role of follicle-stimulating hormone (Fsh) in mediating the effect of clotrimazole on testicular steroidogenesis in adult zebrafish. Toxicology 298: 30–39.

Beer, R. L., and B. W. Draper, 2013 Nanos3 maintains germline stem cells and expression of the conserved germline stem cell gene nanos2 in the zebrafish ovary. Dev. Biol. 374: 308–318.

Bowles, J., D. Knight, C. Smith, D. Wilhelm, J. Richman *et al.*, 2006 Retinoid signaling determines germ cell fate in mice. Science 312: 596–600.

Brion, F., C. R. Tyler, X. Palazzi, B. Laillet, J. M. Porcher *et al.*, 2004 Impacts of 17beta-estradiol, including environmentally relevant concentrations, on reproduction after exposure during embryo-larval-, juvenile- and adult-life stages in zebrafish (*Danio rerio*). Aquat. Toxicol. 68: 193–217.

Buaas, F. W., A. L. Kirsh, M. Sharma, D. J. McLean, J. L. Morris *et al.*, 2004 Plzf is required in adult male germ cells for stem cell self-renewal. Nat. Genet. 36: 647–652.

Chen, S. J., H. F. Zhang, F. H. Wang, W. Zhang, and G. Peng, 2016 nr0b1 (DAX1) mutation in zebrafish causes female-to-male sex reversal through abnormal gonadal proliferation and differentiation. Mol. Cell. Endocrinol. 433: 105–116.

Chen, S. X., J. Bogerd, N. E. Schoonen, J. Martijn, P. P. de Waal *et al.*,2013 A progestin (17alpha,20beta-dihydroxy-4-pregnen-3-one) stimulates early stages of spermatogenesis in zebrafish. Gen. Comp. Endocrinol. 185: 1–9.

de Waal, P. P., D. S. Wang, W. A. Nijenhuis, R. W. Schulz, and J. Bogerd,2008 Functional characterization and expression analysis of the androgen receptor in zebrafish (*Danio rerio*) testis. Reproduction 136: 225–234.

Dimitriadis, F., C. Tsiampali, N. Chaliasos, P. Tsounapi, A. Takenaka *et al.*, 2015 The Sertoli cell as the orchestra conductor of spermatogenesis: spermatogenic cells dance to the tune of testosterone. Hormones (Athens) 14: 479–503.

Dranow, D. B., R. P. Tucker, and B. W. Draper, 2013 Germ cells are required to maintain a stable sexual phenotype in adult zebrafish. Dev. Biol. 376: 43–50.

Dranow, D. B., K. Hu, A. M. Bird, S. T. Lawry, M. T. Adams *et al.*, 2016 Bmp15 is an oocyte-produced signal required for maintenance of the adult female sexual phenotype in zebrafish. PLoS Genet. 12: e1006323.

Gautier, A., F. Sohm, J. S. Joly, F. Le Gac, and J. J. Lareyre, 2011 The proximal promoter region of the zebrafish gsdf gene is sufficient to mimic the spatio-temporal expression pattern of the endogenous gene in Sertoli and granulosa cells. Biol. Reprod. 85: 1240–1251.

Good-Avila, S. V., S. Yegorov, S. Harron, J. Bogerd, P. Glen *et al.*, 2009 Relaxin gene family in teleosts: phylogeny, syntenic mapping, selective constraint, and expression analysis. BMC Evol. Biol. 9: 293.

Gui, J. F., and Z. Y. Zhu, 2012 Molecular basis and genetic improvement of economically important traits in aquaculture animals. Sci. Bull. 57: 1751–1760.

Herpin, A., and M. Schartl, 2015 Plasticity of gene-regulatory networks controlling sex determination: of masters, slaves, usual suspects, newcomers, and usurpators. EMBO Rep. 16: 1260–1274.

Hinfray, N., D. Baudiffier, M. C. Leal, J. M. Porcher, S. Ait-Aissa *et al.*, 2011 Characterization of testicular expression of P450 17alpha-hydroxylase, 17,20-lyase in zebrafish and its perturbation by the pharmaceutical fungicide clotrimazole. Gen. Comp. Endocrinol. 174: 309–317.

Kim, S., V. J. Bardwell, and D. Zarkower, 2007 Cell type-autonomous and non-autonomous requirements for Dmrt1 in postnatal testis differentiation. Dev. Biol. 307: 314–327.

Kimmel, C. B., W. W. Ballard, S. R. Kimmel, B. Ullmann, and T. F. Schilling, 1995 Stages of embryonic development of the zebrafish. Dev. Dyn. 203: 253–310.

Kobayashi, A., C. A. Stewart, Y. Wang, K. Fujioka, N. C. Thomas *et al.*, 2011 β-Catenin is essential for Mullerian duct regression during male sexual differentiation. Development 138: 1967–1975.

Leal, M. C., E. R. Cardoso, R. H. Nobrega, S. R. Batlouni, J. Bogerd *et al.*, 2009 Histological and stereological evaluation of zebrafish (*Danio rerio*) spermatogenesis with an emphasis on spermatogonial generations. Biol. Reprod. 81: 177–187.

Li, M. H., and D. S. Wang, 2017 Gene editing nuclease and its application in tilapia. Sci. Bull. 62: 165–173.

Li, X. Y., Z. Li, X. J. Zhang, L. Zhou, and J. F. Gui, 2014a Expression characterization of testicular DMRT1 in both Sertoli cells and spermatogenic cells of polyploid gibel carp. Gene 548: 119–125.

Li, X. Y., X. J. Zhang, Z. Li, W. Hong, W. Liu *et al.*, 2014b Evolutionary history of two divergent Dmrt1 genes reveals two rounds of polyploidy origins in gibel carp. Mol. Phylogenet. Evol. 78: 96–104.

Li, X. Y., X. L. Liu, M. Ding, Z. Li, L. Zhou *et al.*, 2017 A novel male-specific SET domain-containing gene setdm identified from extra microchromosomes of gibel carp males. Sci. Bull. 62: 528–536.

Liu, W., S. Z. Li, Z. Li, Y. Wang, X. Y. Li *et al.*, 2015 Complete depletion of primordial germ cells in an all-female fish leads to sex-biased gene expression alteration and sterile all-male occurrence. BMC Genomics 16: 971.

Marshall, G. R., D. S. Zorub, and T. M. Plant, 1995 Follicle-stimulating hormone amplifies the population of differentiated spermatogonia in the hypophysectomized testosterone-replaced adult rhesus monkey (*Macaca mulatta*). Endocrinology 136: 3504–3511.

Masuyama, H., M. Yamada, Y. Kamei, T. Fujiwara-Ishikawa, T. Todo *et al.*, 2012 Dmrt1 mutation causes a male-to-female sex reversal after the sex determination by Dmy in the medaka. Chromosome Res. 20: 163–176.

Matson, C. K., and D. Zarkower, 2012 Sex and the singular DM domain: insights into sexual regulation, evolution and plasticity. Nat. Rev. Genet. 13: 163–174.

Matsuda, M., Y. Nagahama, A. Shinomiya, T. Sato, C. Matsuda *et al.*, 2002 DMY is a Y-specific DM-domain gene required for male development in the medaka fish. Nature 417: 559–563.

Mei, J., and J. F. Gui, 2015 Genetic basis and biotechnological manipulation of sexual dimorphism and sex determination in fish. Sci. China Life Sci. 58: 124–136.

Mei, J., Q. Y. Zhang, Z. Li, S. Lin, and J. F. Gui, 2008 C1q-like inhibits p53-mediated apoptosis and controls normal hematopoiesis during zebrafish embryogenesis. Dev. Biol. 319: 273–284.

Meng, X., M. Lindahl, M. E. Hyvonen, M. Parvinen, D. G. de Rooij *et al.*, 2000 Regulation of cell fate decision of undifferentiated spermatogonia by GDNF. Science 287: 1489–1493.

Morinaga, C., D. Saito, S. Nakamura, T. Sasaki, S. Asakawa *et al.*, 2007 The hotei mutation of medaka in the anti-Mullerian hormone receptor causes the dysregulation of germ cell and sexual development. Proc. Natl. Acad. Sci. USA 104: 9691–9696.

Nakamura, S., D. Kobayashi, Y. Aoki, H. Yokoi, Y. Ebe *et al.*, 2006 Identification and lineage tracing of two populations of somatic gonadal precursors in medaka embryos. Dev. Biol. 295: 678–688.

Nakamura, S., I. Watakabe, T. Nishimura, J. Y. Picard, A. Toyoda *et al.*, 2012 Hyperproliferation of mitotically active germ cells due to defective anti-Mullerian hormone signaling mediates sex reversal in medaka. Development 139: 2283–2287.

Neumann, J. C., G. L. Chandler, V. A. Damoulis, N. J. Fustino, K. Lillard *et al.*, 2011 Mutation in the type IB bone morphogenetic protein receptor Alk6b impairs germ-cell differentiation and causes germ-cell tumors in zebrafish. Proc. Natl. Acad. Sci. USA 108: 13153–13158.

Orban, L., R. Sreenivasan, and P. E. Olsson, 2009 Long and winding roads: testis differentiation in zebrafish. Mol. Cell. Endocrinol. 312: 35–41.

Ozaki, Y., K. Saito, M. Shinya, T. Kawasaki, and N. Sakai, 2011 Evaluation of Sycp3, Plzf and Cyclin B3 expression and suitability as spermatogonia and spermatocyte markers in zebrafish. Gene Expr. Patterns 11: 309–315.

Peng, J. X., J. L. Xie, L. Zhou, Y. H. Hong, and J. F. Gui, 2009 Evolutionary conservation of Dazl genomic organization and its continuous and dynamic distribution throughout germline development in gynogenetic gibel carp. J. Exp. Zool. B Mol. Dev. Evol. 312: 855–871.

Rocha, A., S. Zanuy, and A. Gomez, 2016 Conserved anti-Mullerian hormone: anti-Mullerian hormone type-2 receptor specific interaction and intracellular signaling in teleosts. Biol. Reprod. 94: 141.

Rodríguez-Marí, A., Y. L. Yan, R. A. Bremiller, C. Wilson, C. Cañestro *et al.*, 2005 Characterization and expression pattern of zebrafish anti-Mullerian hormone (Amh) relative to sox9a, sox9b, and cyp19a1a, during gonad development. Gene Expr. Patterns 5: 655–667.

Rodríguez-Marí, A., C. Cañestro, R. A. BreMiller, A. Nguyen-Johnson, K. Asakawa *et al.*, 2010 Sex reversal in zebrafish fancl mutants is caused by Tp53-mediated germ cell apoptosis. PLoS Genet. 6: e1001034.

Rodríguez-Marí, A., C. Wilson, T. A. Titus, C. Cañestro, R. A. BreMiller *et al.*, 2011 Roles of brca2 (fancd1) in oocyte nuclear architecture, gametogenesis, gonad tumors, and genome stability in zebrafish. PLoS Genet. 7: e1001357.

Rossitto, M., P. Philibert, F. Poulat, and B. Boizet-Bonhoure, 2015 Molecular events and signalling pathways of male germ cell differentiation in mouse. Semin. Cell Dev. Biol. 45: 84–93.

Saitou, M., 2009 Germ cell specification in mice. Curr. Opin. Genet. Dev. 19: 386–395.

Skaar, K. S., R. H. Nobrega, A. Magaraki, L. C. Olsen, R. W. Schulz *et al.*, 2011 Proteolytically activated, recombinant anti-Mullerian hormone inhibits androgen secretion, proliferation, and differentiation of spermatogonia in adult zebrafish testis organ cultures. Endocrinology 152: 3527–3540.

Slanchev, K., J. Stebler, G. de la Cueva-Mendez, and E. Raz, 2005 Development without germ cells: the role of the germ line in zebrafish sex differentiation. Proc. Natl. Acad. Sci. USA 102: 4074–4079.

Sun, D., Y. Zhang, C. Wang, X. Hua, X. A. Zhang *et al.*, 2013 Sox9-related signaling controls zebrafish juvenile ovary-testis transformation. Cell Death Dis. 4: e930.

Sun, H. Y., G. M. Zhang, F. L. Dong, F. Wang, and W. G. Cao, 2014 Reprogramming Sertoli cells into pluripotent stem cells. Cell. Reprogram. 16: 196–205.

Sweeney, S. T., A. Hidalgo, J. S. de Belle, and H. Keshishian, 2012 TUNEL-antibody double-labeling method for *Drosophila* embryos. Cold Spring Harb. Protoc. 2012: 1013–1016.

Tsuda, M., Y. Sasaoka, M. Kiso, K. Abe, S. Haraguchi *et al.*, 2003 Conserved role of nanos proteins in germ cell development. Science 301: 1239–1241.

Wang, H., L. Wen, Q. Yuan, M. Sun, M. Niu *et al.*, 2016 Establishment and applications of male germ cell and Sertoli cell lines. Reproduction 152: R31–R40.

Wang, X. G., and L. Orban, 2007 Anti-Mullerian hormone and 11 beta-hydroxylase show reciprocal expression to that of aromatase in the transforming gonad of zebrafish males. Dev. Dyn. 236: 1329–1338.

Wang, X. G., R. Bartfai, I. Sleptsova-Freidrich, and L. Orban, 2007 The timing and extent of 'juvenile ovary' phase are highly variable during zebrafish testis differentiation. J. Fish Biol. 70: 33–44.

Wang, Y., L. Zhou, B. Yao, C. J. Li, and J. F. Gui, 2004 Differential expression of thyroid-stimulating hormone beta subunit in gonads during sex reversal of orange-spotted and red-spotted groupers. Mol. Cell. Endocrinol. 220: 77–88.

Wang, Y., L. Zhou, Z. Li, W. H. Li, and J. F. Gui, 2013 Apolipoprotein C1 regulates epiboly during gastrulation in zebrafish. Sci. China Life Sci. 56: 975–984.

Webster, K. A., U. Schach, A. Ordaz, J. S. Steinfeld, B. W. Draper *et al.*, 2017 Dmrt1 is necessary for male sexual development in zebrafish. Dev. Biol. 422: 33–46.

Weidinger, G., J. Stebler, K. Slanchev, K. Dumstrei, C. Wise *et al.*, 2003 Dead end, a novel vertebrate germ plasm component, is required for zebrafish primordial germ cell migration and survival. Curr. Biol. 13: 1429–1434.

Westerfield, M., 2000 *The Zebrafish Book: A Guide for the Laboratory Use of Zebrafish (Danio rerio)*. University of Oregon Press, Eugene, OR.

Xia, W., L. Zhou, B. Yao, C. J. Li, and J. F. Gui, 2007 Differential and spermatogenic cell-specific expression of DMRT1 during sex reversal in protogynous hermaphroditic groupers. Mol. Cell. Endocrinol. 263: 156–172.

Xiong, S. T., J. J. Wu, J. Jing, P. P. Huang, Z. Li *et al.*, 2017 Loss of stat3 function leads to spine malformation and immune disorder in zebrafish. Sci. Bull. 62: 185–196.

Xu, H. Y., M. Y. Li, J. F. Gui, and Y. H. Hong, 2010 Fish germ cells. Sci. China Life Sci. 53: 435–446.

Yang, Y. J., Y. Wang, Z. Li, L. Zhou, and J. F. Gui, 2017 Sequential, divergent, and cooperative requirements of foxl2a and foxl2b in ovary development and maintenance of zebrafish. Genetics 205: 1551–1572.

Yoon, C., K. Kawakami, and N. Hopkins, 1997 Zebrafish vasa homologue RNA is localized to the cleavage planes of 2- and 4-cell-stage embryos and is expressed in the primordial germ cells. Development 124: 3157–3165.

Zhang, L. J., M. Chen, Q. Wen, Y. Q. Li, Y. Q. Wang *et al.*, 2015a Reprogramming of Sertoli cells to fetal-like Leydig cells by Wt1 ablation. Proc. Natl. Acad. Sci. USA 112: 4003–4008.

Zhang, T., J. Oatley, V. J. Bardwell, and D. Zarkower, 2016 DMRT1 is required for mouse spermatogonial stem cell maintenance and replenishment. PLoS Genet. 12: e1006293.

Zhang, Z. W., S. W. Lau, L. L. Zhang, and W. Ge, 2015b Disruption of zebrafish follicle-stimulating hormone receptor (fshr) but not luteinizing hormone receptor (lhcgr) gene by TALEN leads to failed follicle activation in females followed by sexual reversal to males. Endocrinology 156: 3747–3762.

Communicating editor: D. Parichy